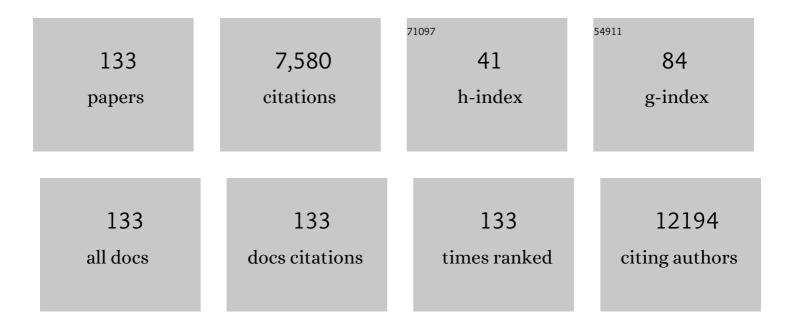
List of Publications by Year in descending order

Source: https://exaly.com/author-pdf/1555043/publications.pdf Version: 2024-02-01



#	Article	IF	CITATIONS
1	Bandgap Engineering of Strained Monolayer and Bilayer MoS ₂ . Nano Letters, 2013, 13, 3626-3630.	9.1	1,950
2	Probing excitonic states in suspended two-dimensional semiconductors by photocurrent spectroscopy. Scientific Reports, 2014, 4, 6608.	3.3	351
3	Chemical origin of a graphene moiré overlayer on Ru(0001). Physical Chemistry Chemical Physics, 2008, 10, 3530.	2.8	242
4	Role of Defects in the Phase Transition of VO ₂ Nanoparticles Probed by Plasmon Resonance Spectroscopy. Nano Letters, 2012, 12, 780-786.	9.1	196
5	Comparison of electronic structure and template function of single-layer graphene and a hexagonal boron nitride nanomesh on Ru(0001). Physical Review B, 2009, 79, .	3.2	186
6	Scalable Synthesis of Uniform Few-Layer Hexagonal Boron Nitride Dielectric Films. Nano Letters, 2013, 13, 276-281.	9.1	186
7	Structure Determination of the Coincidence Phase of Graphene on Ru(0001). Physical Review Letters, 2010, 104, 136102.	7.8	185
8	Solvent-mediated charge separation drives alternative hydrogenation path of furanics in liquid water. Nature Catalysis, 2019, 2, 431-436.	34.4	171
9	Water-Mediated Heterogeneously Catalyzed Reactions. ACS Catalysis, 2020, 10, 1294-1309.	11.2	156
10	C–C Coupling on Single-Atom-Based Heterogeneous Catalyst. Journal of the American Chemical Society, 2018, 140, 954-962.	13.7	142
11	Graphene Oxideâ€Template Controlled Cuboidâ€Shaped Highâ€Capacity VS ₄ Nanoparticles as Anode for Sodiumâ€Ion Batteries. Advanced Functional Materials, 2018, 28, 1801806.	14.9	125
12	Ultrafast Phase Transition via Catastrophic Phonon Collapse Driven by Plasmonic Hot-Electron Injection. Nano Letters, 2014, 14, 1127-1133.	9.1	123
13	Probing charge scattering mechanisms in suspended graphene by varying its dielectric environment. Nature Communications, 2012, 3, 734.	12.8	119
14	Formation of Large Polysulfide Complexes during the Lithium-Sulfur Battery Discharge. Physical Review Applied, 2014, 2, .	3.8	105
15	Periodicity, work function and reactivity of graphene on Ru(0001) from first principles. New Journal of Physics, 2010, 12, 043041.	2.9	104
16	Controlling Reaction Selectivity over Hybrid Plasmonic Nanocatalysts. Nano Letters, 2018, 18, 7289-7297.	9.1	92
17	Enhanced NH 3 -sensing behavior of 2,9,16,23-tetrakis(2,2,3,3-tetrafluoropropoxy) metal(II) phthalocyanine/multi-walled carbon nanotube hybrids: An investigation of the effects of central metals. Carbon, 2014, 80, 268-278.	10.3	84
18	Zeolite-catalysed C–C bond forming reactions for biomass conversion to fuels and chemicals. Catalysis Science and Technology, 2016, 6, 2543-2559.	4.1	84

#	Article	IF	CITATIONS
19	Structure and Catalytic Characterization of a Second Framework Al(IV) Site in Zeolite Catalysts Revealed by NMR at 35.2 T. Journal of the American Chemical Society, 2020, 142, 7514-7523.	13.7	78
20	Strain enhanced defect reactivity at grain boundaries in polycrystalline graphene. Carbon, 2011, 49, 3983-3988.	10.3	74
21	Gas transport in porous electrodes of solid oxide fuel cells: A review on diffusion and diffusivity measurement. Journal of Power Sources, 2013, 237, 64-73.	7.8	73
22	Arrays of Ru nanoclusters with narrow size distribution templated by monolayer graphene on Ru. Surface Science, 2011, 605, 1676-1684.	1.9	70
23	Single Terrace Growth of Graphene on a Metal Surface. Nano Letters, 2011, 11, 1895-1900.	9.1	68
24	Relationship between Atomic Scale Structure and Reactivity of Pt Catalysts: Hydrodeoxygenation of <i>m</i> -Cresol over Isolated Pt Cations and Clusters. ACS Catalysis, 2020, 10, 595-603.	11.2	68
25	Controllable healing of defects and nitrogen doping of graphene by CO and NO molecules. Physical Review B, 2011, 83, .	3.2	67
26	Distributed processes for biomass conversion could aid UN Sustainable Development Goals. Nature Catalysis, 2018, 1, 731-735.	34.4	66
27	Monolayer Graphene and <i>h</i> -BN on Metal Substrates as Versatile Templates for Metallic Nanoclusters. Journal of Physical Chemistry Letters, 2011, 2, 2341-2345.	4.6	63
28	Defects and doping and their role in functionalizing graphene. MRS Bulletin, 2012, 37, 1187-1194.	3.5	61
29	Tuning the spin state of iron phthalocyanine by ligand adsorption. Journal of Physics Condensed Matter, 2010, 22, 472002.	1.8	59
30	Low-Energy X-ray and Ozone-Exposure Induced Defect Formation in Graphene Materials and Devices. IEEE Transactions on Nuclear Science, 2011, 58, 2961-2967.	2.0	56
31	Simulation of high-energy ion collisions with graphene fragments. Physical Review B, 2012, 85, .	3.2	56
32	Gel based sulfur cathodes with a high sulfur content and large mass loading for high-performance lithium–sulfur batteries. Journal of Materials Chemistry A, 2017, 5, 1650-1657.	10.3	56
33	Enhanced Electrochemical and Thermal Transport Properties of Graphene/MoS ₂ Heterostructures for Energy Storage: Insights from Multiscale Modeling. ACS Applied Materials & Interfaces, 2018, 10, 14614-14621.	8.0	56
34	Confining Sulfur Species in Cathodes of Lithium–Sulfur Batteries: Insight into Nonpolar and Polar Matrix Surfaces. ACS Energy Letters, 2016, 1, 481-489.	17.4	53
35	Substitutional doping of graphene: The role of carbon divacancies. Physical Review B, 2014, 89, .	3.2	52
36	Direct quantitative identification of the "surface trans-effect― Chemical Science, 2016, 7, 5647-5656.	7.4	51

#	Article	IF	CITATIONS
37	Comparison of the Carbonyl and Nitrosyl Complexes Formed by Adsorption of CO and NO on Monolayers of Iron Phthalocyanine on Au(111). Journal of Physical Chemistry C, 2011, 115, 24718-24727.	3.1	49
38	Graphene on Ru(0001): Contact Formation and Chemical Reactivity on the Atomic Scale. Physical Review Letters, 2010, 105, 236101.	7.8	48
39	Magnetic moment of a single vacancy in graphene and semiconducting nanoribbons. Physical Review B, 2012, 86, .	3.2	45
40	Direct carbon-carbon coupling of furanics with acetic acid over Brønsted zeolites. Science Advances, 2016, 2, e1601072.	10.3	44
41	Photoresponse of Natural van der Waals Heterostructures. ACS Nano, 2017, 11, 6024-6030.	14.6	44
42	Ammonia adsorption on iron phthalocyanine on Au(111): Influence on adsorbate–substrate coupling and molecular spin. Journal of Chemical Physics, 2011, 134, 114710.	3.0	40
43	Reaction of Phthalocyanines with Graphene on Ir(111). Journal of the American Chemical Society, 2015, 137, 9452-9458.	13.7	40
44	Introduction of nitrogen with controllable configuration into graphene via vacancies and edges. Journal of Materials Chemistry A, 2013, 1, 14927.	10.3	39
45	Ozone-exposure and annealing effects on graphene-on-SiO2 transistors. Applied Physics Letters, 2012, 101, .	3.3	38
46	Suppression of phononâ€mediated hot carrier relaxation in typeâ€II InAs/AlAs _{<i>x</i>} Sb _{1 â°' <i>x</i>} quantum wells: a practical route to hot carrier solar cells. Progress in Photovoltaics: Research and Applications, 2016, 24, 591-599.	8.1	38
47	Role of water in cyclopentanone self-condensation reaction catalyzed by MCM-41 functionalized with sulfonic acid groups. Journal of Catalysis, 2019, 377, 245-254.	6.2	38
48	Aldol Condensation of Cyclopentanone on Hydrophobized MgO. Promotional Role of Water and Changes in the Rate-Limiting Step upon Organosilane Functionalization. ACS Catalysis, 2019, 9, 2831-2841.	11.2	38
49	Enhanced hot electron lifetimes in quantum wells with inhibited phonon coupling. Scientific Reports, 2018, 8, 12473.	3.3	37
50	BrÃ,nsted–BrÃ,nsted Synergies between Framework and Noncrystalline Protons in Zeolite H-ZSM-5. ACS Catalysis, 2019, 9, 6124-6136.	11.2	37
51	Understanding the Different Diffusion Mechanisms of Hydrated Protons and Potassium Ions in Titanium Carbide MXene. ACS Applied Materials & Interfaces, 2019, 11, 7087-7095.	8.0	36
52	An analytical expression for the van der Waals interaction in oriented-attachment growth: a spherical nanoparticle and a growing cylindrical nanorod. Physical Chemistry Chemical Physics, 2012, 14, 4548.	2.8	35
53	Strain engineering of two-dimensional materials for advanced electrocatalysts. Materials Today Nano, 2021, 14, 100111.	4.6	35
54	Pyridine Adsorption on Single-Layer Iron Phthalocyanine on Au(111). Journal of Physical Chemistry C, 2011, 115, 20201-20208.	3.1	34

#	Article	IF	CITATIONS
55	Hydrogen dynamics and metallic phase stabilization in VO2. Applied Physics Letters, 2014, 104, .	3.3	34
56	First-Principles Study on the Structure, Electronic, and Optical Properties of Cs ₂ AgBiBr _{6-x} Cl _{<i>x</i>} Mixed-Halide Double Perovskites. Journal of Physical Chemistry C, 2020, 124, 5371-5377.	3.1	34
57	Reaction Pathway Dependence in Plasmonic Catalysis: Hydrogenation as a Model Molecular Transformation. Chemistry - A European Journal, 2018, 24, 12330-12339.	3.3	33
58	Layer-Dependent Interfacial Transport and Optoelectrical Properties of MoS ₂ on Ultraflat Metals. ACS Applied Materials & Interfaces, 2019, 11, 31543-31550.	8.0	33
59	Thermal Unequilibrium of PdSn Intermetallic Nanocatalysts: From In Situ Tailored Synthesis to Unexpected Hydrogenation Selectivity. Angewandte Chemie - International Edition, 2021, 60, 18309-18317.	13.8	32
60	Structure, electronic and optical properties of CsPbX3 halide perovskite: A first-principles study. Journal of Alloys and Compounds, 2021, 862, 158442.	5.5	31
61	Solvent effects on catalytic reactions and related phenomena at liquid-solid interfaces. Surface Science Reports, 2021, 76, 100541.	7.2	31
62	Electron spectroscopy study of the initial stages of iron phthalocyanine growth on highly oriented pyrolitic graphite. Journal of Chemical Physics, 2009, 131, 214709.	3.0	29
63	A Multisensor Device for Highly Efficient Diffusivity Measurements and Overall oncentrationâ€Polarization Evaluation in Fuel Cells. Advanced Energy Materials, 2012, 2, 329-333.	19.5	29
64	Interaction of water with zeolites: a review. Catalysis Reviews - Science and Engineering, 2021, 63, 302-362.	12.9	28
65	Comment on "Periodically Rippled Graphene: Growth and Spatially Resolved Electronic Structureâ€. Physical Review Letters, 2008, 101, 099703; author reply 099704.	7.8	27
66	Enhanced chemical reactions of oxygen at grain boundaries in polycrystalline graphene. Polyhedron, 2013, 64, 158-162.	2.2	27
67	Total Ionizing Dose Effects on hBN Encapsulated Graphene Devices. IEEE Transactions on Nuclear Science, 2014, 61, 2868-2873.	2.0	27
68	Transition metal-like carbocatalyst. Nature Communications, 2020, 11, 4091.	12.8	27
69	Overall concentration polarization and limiting current density of fuel cells with nanostructured electrodes. Nano Energy, 2012, 1, 828-832.	16.0	26
70	Water Promotion (or Inhibition) of Condensation Reactions Depends on Exposed Cerium Oxide Catalyst Facets. ACS Catalysis, 2020, 10, 5373-5382.	11.2	25
71	Photoinduced Electron and Energy Transfer Pathways and Photocatalytic Mechanisms in Hybrid Plasmonic Photocatalysis. Advanced Optical Materials, 2021, 9, 2101128.	7.3	25
72	Physical justification for ionic conductivity enhancement at strained coherent interfaces. Journal of Power Sources, 2015, 285, 37-42.	7.8	23

#	Article	IF	CITATIONS
73	Homogeneous <i>versus</i> heterogeneous catalysis in Cu ₂ O-nanoparticle-catalyzed C–C coupling reactions. Green Chemistry, 2019, 21, 5284-5290.	9.0	23
74	Quantifying the Influence of Water on the Mobility of Aluminum Species and Their Effects on Alkane Cracking in Zeolites. ACS Catalysis, 2021, 11, 6982-6994.	11.2	23
75	Interfacial coupling in rotational monolayer and bilayer graphene on Ru(0001) from first principles. Nanoscale, 2012, 4, 4687.	5.6	20
76	Electrical Stress and Total Ionizing Dose Effects on <formula formulatype="inline"><tex Notation="TeX">\${hbox {MoS}}_{2}\$ </tex </formula> Transistors. IEEE Transactions on Nuclear Science, 2014, 61, 2862-2867.	2.0	20
77	Visualization of Defect-Induced Excitonic Properties of the Edges and Grain Boundaries in Synthesized Monolayer Molybdenum Disulfide. Journal of Physical Chemistry C, 2016, 120, 24080-24087.	3.1	20
78	Enhancing the Acylation Activity of Acetic Acid by Formation of an Intermediate Aromatic Ester. ChemSusChem, 2017, 10, 2823-2832.	6.8	20
79	Enhanced chemical activity and wettability at adjacent BrÃ,nsted acid sites in HZSM-5. Catalysis Today, 2018, 312, 44-50.	4.4	20
80	Design-controlled synthesis of IrO ₂ sub-monolayers on Au nanoflowers: marrying plasmonic and electrocatalytic properties. Nanoscale, 2020, 12, 12281-12291.	5.6	20
81	High-Temperature Grafting Silylation for Minimizing Leaching of Acid Functionality from Hydrophobic Mesoporous Silicas Used as Catalysts in the Liquid Phase. Langmuir, 2019, 35, 6838-6852.	3.5	19
82	Stabilization of furanics to cyclic ketone building blocks in the vapor phase. Applied Catalysis B: Environmental, 2019, 254, 491-499.	20.2	19
83	Room-Temperature Reactions for Self-Cleaning Molecular Nanosensors. Nano Letters, 2013, 13, 798-802.	9.1	18
84	Adsorption of ammonia on multilayer iron phthalocyanine. Journal of Chemical Physics, 2011, 134, 114711.	3.0	17
85	Hydrodeoxygenation of anisole over different Rh surfaces. Chinese Journal of Catalysis, 2019, 40, 1721-1730.	14.0	17
86	Metal–organic interaction probed by First Principles STM simulations. Progress in Surface Science, 2010, 85, 435-459.	8.3	16
87	Doubling the diffusivity measurement efficiency in solid oxide fuel cells (SOFCs) via a bi-sensor electrochemical cell. Journal of Power Sources, 2011, 196, 9985-9988.	7.8	15
88	Efficient catalytic dehydration of methyl lactate to acrylic acid using sulphate and phosphate modified MCM-41 catalysts. Applied Catalysis A: General, 2014, 487, 219-225.	4.3	15
89	Growth of Solid and Hollow Gold Particles through the Thermal Annealing of Nanoscale Patterned Thin Films. ACS Applied Materials & Interfaces, 2013, 5, 11590-11596.	8.0	14
90	A comparative study of thermal- and electrocatalytic conversion of furfural: methylfuran as a primary and major product. Journal of Applied Electrochemistry, 2021, 51, 19-26.	2.9	14

#	Article	IF	CITATIONS
91	Plasmon-Induced CO ₂ Conversion on Al@Cu ₂ O: A DFT Study. Journal of Physical Chemistry C, 2021, 125, 6108-6115.	3.1	14
92	Optimizing the surface distribution of acid sites for cooperative catalysis in condensation reactions promoted by water. Chem Catalysis, 2021, 1, 1065-1087.	6.1	14
93	General Synthetic Strategy to Ordered Mesoporous Carbon Catalysts with Singleâ€Atom Metal Sites for Electrochemical CO ₂ Reduction. Small, 2022, 18, e2107799.	10.0	13
94	Ionization-Enhanced Decomposition of 2,4,6-Trinitrotoluene (TNT) Molecules. Journal of Physical Chemistry A, 2011, 115, 8142-8146.	2.5	12
95	Surface Reactions and Defect Formation in Irradiated Graphene Devices. IEEE Transactions on Nuclear Science, 2012, 59, 3039-3044.	2.0	12
96	Reaction Mechanism for the Conversion of γ-Valerolactone (GVL) over a Ru Catalyst: A First-Principles Study. Industrial & Engineering Chemistry Research, 2017, 56, 3217-3222.	3.7	12
97	Predictors of unfavorable outcome in neurosyphilis: Multicenter ID-IRI Study. European Journal of Clinical Microbiology and Infectious Diseases, 2019, 38, 125-134.	2.9	12
98	Analysis and visualization of energy densities. II. Insights from linear-response time-dependent density functional theory calculations. Physical Chemistry Chemical Physics, 2020, 22, 26852-26864.	2.8	12
99	Templating of arrays of Ru nanoclusters by monolayer graphene/Ru Moirés with different periodicities. Journal of Physics Condensed Matter, 2012, 24, 314201.	1.8	11
100	The Effect of Cofed Species on the Kinetics of Catalytic Methyl Lactate Dehydration on NaY. ACS Catalysis, 2018, 8, 9066-9078.	11.2	11
101	The effect and nature of N–H complexes in the control of the dominant photoluminescence transitions in UV-hydrogenated GalnNAs. RSC Advances, 2017, 7, 25353-25361.	3.6	10
102	Rational Surface Modification of Two-Dimensional Layered Black Phosphorus: Insights from First-Principles Calculations. ACS Omega, 2018, 3, 2445-2451.	3.5	10
103	Ab initio calculations of ionic hydrocarbon compounds with heptacoordinate carbon. Journal of Molecular Modeling, 2018, 24, 116.	1.8	10
104	Factors Determining Selectivity of Acid- and Base-Catalyzed Self- and Cross-Condensation of Acetone and Cyclopentanone. ACS Catalysis, 2020, 10, 12790-12800.	11.2	10
105	First-Principles Study on the Structure, Electronic and Optical Properties of Cs ₂ AgSb _{<i>x</i>} Bi _{1â€⁴<i>x</i>} Cl ₆ Double Perovskites. Journal of Physical Chemistry C, 2021, 125, 11271-11277.	3.1	10
106	A current-sensor electrochemical device for accurate gas diffusivity measurement in fuel cells. Journal of Power Sources, 2013, 232, 93-98.	7.8	9
107	Analysis and visualization of energy densities. I. Insights from real-time time-dependent density functional theory simulations. Physical Chemistry Chemical Physics, 2020, 22, 26838-26851.	2.8	9
108	Oxide-catalyzed self- and cross-condensation of cycloketones. Kinetically relevant steps that determine product distribution. Journal of Catalysis, 2020, 391, 163-174.	6.2	9

#	Article	IF	CITATIONS
109	Enhanced photoresponse in curled graphene ribbons. Nanoscale, 2013, 5, 12206.	5.6	8
110	Doping-driven electronic and lattice dynamics in the phase-change material vanadium dioxide. Physical Review B, 2020, 102, .	3.2	8
111	Selective Reduction of Carboxylic Acids to Aldehydes with Promoted MoO ₃ Catalysts. ACS Catalysis, 2022, 12, 6313-6324.	11.2	8
112	Thermal Unequilibrium of PdSn Intermetallic Nanocatalysts: From In Situ Tailored Synthesis to Unexpected Hydrogenation Selectivity. Angewandte Chemie, 2021, 133, 18457-18465.	2.0	7
113	First-Formed Framework Species and Phosphate Structure Distributions in Phosphorus-Modified MFI Zeolites. Journal of Physical Chemistry C, 2022, 126, 227-238.	3.1	7
114	Significant Role of Oxygen Dopants in Photocatalytic PFCA Degradation over h-BN. ACS Applied Materials & Interfaces, 2021, 13, 46727-46737.	8.0	6
115	Nondestructive functionalization of monolayer black phosphorus using Lewis acids: A first-principles study. Applied Surface Science, 2020, 518, 146210.	6.1	6
116	First-principles calculations of the structural, electronic and optical properties of Cs2AgxNa1-xInBr6 double perovskites. Chemical Physics, 2022, 559, 111520.	1.9	6
117	Proton shuttling flattens the energy landscape of nitrite catalytic reduction. Journal of Catalysis, 2022, 413, 252-263.	6.2	6
118	Experimental and computational kinetics study of the liquid-phase hydrogenation of C C and C O bonds. Journal of Catalysis, 2021, 404, 771-785.	6.2	5
119	Role of In in Hydrogenation of N-Related Complexes in GaInNAs. ACS Applied Electronic Materials, 2019, 1, 461-466.	4.3	4
120	Plasmonic photocatalysis. Catalysis, 2021, , 38-86.	1.0	4
121	Voltage-dependent conductance states of a single-molecule junction. Journal of Physics Condensed Matter, 2012, 24, 394012.	1.8	2
122	Interfacial engineering of phthalocyanine molecules on graphitic and metal substrates. Molecular Simulation, 2017, 43, 384-393.	2.0	2
123	Localized Orbital Excitation Drives Bond Formation in Plasmonic Catalysis. ACS Applied Materials & Interfaces, 2021, 13, 60115-60124.	8.0	2
124	Giant Effects of Interlayer Interaction on Valence-Band Splitting in Transition Metal Dichalcogenides. Journal of Physical Chemistry C, 2022, 126, 8667-8675.	3.1	2
125	Physical and Chemical Properties of Phosphorus. ACS Symposium Series, 2019, , 61-77.	0.5	1
126	First-Principles Study of Interaction between Molecules and Lewis Acid Zeolites Manipulated by Injection of Energized Charge Carriers. Industrial & Engineering Chemistry Research, 2021, 60, 14124-14133.	3.7	1

#	Article	IF	CITATIONS
127	Correction: Analysis and visualization of energy densities. I. Insights from real-time time-dependent density functional theory simulations. Physical Chemistry Chemical Physics, 2021, 23, 8936-8936.	2.8	1
128	(Invited) Doping, Functionalization, and Permeability of Graphene: Insights from First-Principles Studies. ECS Transactions, 2014, 64, 121-125.	0.5	0
129	Doping-controlled Coherent Electron-Phonon Coupling in Vanadium Dioxide. , 2015, , .		Ο
130	Effect of Alignment on Thermal Conductivity Enhancement of Polyethylene/Graphene Nanoplatelet Composite Materials. , 2016, , .		0
131	Evidence of suppressed hot carrier relaxation in type-II InAs/AlAs1-xSbx quantum wells. , 2016, , .		0
132	The role of N-H complexes in the control of localized center recombination in hydrogenated GaInNAs (Conference Presentation). , 2017, , .		0
133	Control of hot carrier thermalization in type-II quantum wells: a route to practical hot carrier solar cells. , 2018, , .		0